Determination of new sites for two Fe^{3+} EPR centres in $KTiOPO_4$

1995 J. Phys.: Condens. Matter 7 9615

(http://iopscience.iop.org/0953-8984/7/49/023)

J. Phys.: Condens. Matter 7 (1995) 9615–9623. Printed in the UK

Determination of new sites for two Fe^{3+} EPR centres in $KTiOPO_4$

Sang Won Ahn†§, Sung Ho Choh† and Byung Chun Choi‡

† Department of Physics, Korea University, Seoul 136-701, Republic of Korea

‡ Department of Natural Sciences, Pusan National University of Technology, Pusan 608-739, Republic of Korea

Received 20 March 1995, in final form 4 September 1995

Abstract. EPR spectra of Fe^{3+} ions in single crystals of $KTiOPO_4$ (KTP), synthesized by the flux method, have been investigated at room temperature by employing a Bruker Q-band spectrometer. From the angular dependence of the EPR spectra, two Fe^{3+} centres denoted as C1 and C2 have been identified, in agreement with the previous analysis by other investigators. In this study, for the first time we have fully identified two groups of four magnetically inequivalent Fe^{3+} sites each belonging to the centres C1 and C2. Two sets of triclinic spin-Hamiltonian parameters, which simultaneously fitted EPR data for the four sites belonging to the centres C1 and C2, were determined. The direction cosines of the principal axes of the **g**-tensor as well as the second-order zero-field splitting (ZFS) tensor are found to be given by the relations: lmn, $\bar{l}mn$, $l\bar{m}n$, and $\bar{l}\bar{m}n$ for each four Fe^{3+} sites of C1 as well as C2, respectively, consistent with the crystallographic point group $mm2$ of KTP.

1. Introduction

Potassium titanium phosphate $KTiOPO_4$ (KTP) is a relatively new, efficient, and promising nonlinear optical material [1]. The EPR study of the Fe^{3+} ion in KTP was initiated by Nizamutdinova *et al* [2]. Stenger *et al* [3] and Gaite *et al* [4] identified four Fe^{3+} centres named ST1, ST2, ST3 and ST4. Although the centre reported by Nizamutdinova *et al* [2] is very similar to ST2 and ST4 [4], it has no correspondence with them. There are four chemically equivalent but magnetically inequivalent Ti(1) and Ti(2) sites per unit cell in KTP [5]. EPR studies of other defect centres associated with the four magnetically inequivalent sites have been made [6–9]. However, it appears that no study has been made to identify fully the four magnetically inequivalent Fe^{3+} sites arising from the point symmetry $mm2$ of KTP. This is a comprehensive analysis of the Fe^{3+} EPR of our earlier preliminary report [10].

In the present work, for the first time we have fully identified four magnetically inequivalent Fe^{3+} sites for two EPR centres denoted as C1 and C2, as in our previous work on Cr^{3+} in KTP [9]. The centres C1 and C2 are found to be equivalent to ST3 and ST2, respectively [4]. The four Fe^{3+} centres in our earlier report [10] are equivalent to C2. For the four sites belonging to each centre, C1 and C2, the principal values of the **g**-tensor and the second-order zero-field splitting (ZFS) tensor, and the orientations of their principal axes were determined. The four chemically equivalent but magnetically inequivalent Fe^{3+} sites for each centre are also assigned to the KTP lattice.

§ Present address: Department of Physics and Materials Science, City University of Hong Kong, Kowloon, Hong Kong.

0953-8984/95/499615+09$19.50

2. Experimental procedure

2.1. Sample preparation and crystallography

KTP crystals doped with 0.01 mol% of Fe were grown by the flux method using the chemical $K_6P_4O_{13}$ known [11] as a particularly suitable flux for growing KTP single crystals [10, 12]. The crystal structure of KTP is orthorhombic and belongs to the point group $mm2$ (space group $Pna2_1$) with eight formula units per unit cell, and the details are well established [5, 9]. The structure exhibits two crystallographically different Ti sites: Ti(1) and Ti(2). Both sites lie in slightly distorted oxygen octahedra with local site symmetry C_1, and exhibit approximately the same bond lengths and angles within each TiO_6 complex.

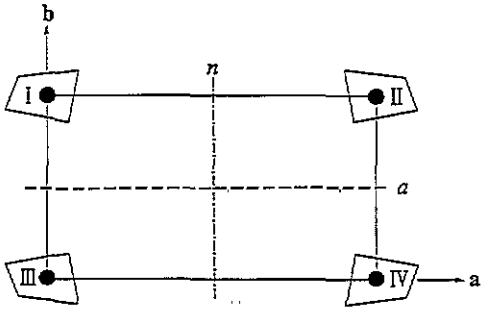

Figure 1. The symmetry relations among the four crystallographically equivalent Ti^{4+} positions in $KTiOPO_4$.

The point symmetry relations among the Ti^{4+} positions in KTP are described in figure 1, where there are four chemically equivalent but magnetically inequivalent Ti sites per unit cell [9]. Position II can be obtained from I by applying a reflection of the glide plane n, perpendicular to the a-axis with subsequent translations of half the lattice constant along the b- and c-axes. Position III can be generated by applying a reflection of the glide plane a (to I), perpendicular to the b-axis with a translation of half the lattice constant along the a-axis. The position IV can be obtained by successively applying the reflections of both glide planes, or applying a rotation around the screw axis 2_1 (to I), which is a 180° rotation around the c-axis with a translation of half the lattice constant along the c-axis. However, when the magnetic field is aligned in any crystallographic plane, the distinction of the lattice translations in the space group $Pna2_1$ can be ignored. This gives rise to some degenerate aspects of the EPR lines [9].

2.2. EPR measurements and spectra details

EPR measurements have been carried out at room temperature by employing a Bruker Q-band spectrometer (ESP 300 series) with 100 kHz modulation at the Seoul Branch of the Korea Basic Science Institute. The microwave frequency was calibrated using the resonance magnetic field of DPPH, where the magnetic field scale at 1.2000 T was calibrated using a Bruker NMR gaussmeter. During the measurements the frequencies were kept within a range of ±0.0003 GHz at 33.8673, 33.8647, and 33.8616 GHz in the ab-, bc- and ca-planes, respectively.

Since the angular dependence of the Fe^{3+} spectra varied by up to 30 mT per degree and the EPR lines were split by small deviations of the crystal alignment from the exact

orientation, it was crucial to make an accurate crystal mounting in order to obtain good angular dependence. The crystal was oriented by the x-ray Laue method, and mounted inside the cylindrical cavity in such a way that each crystallographic plane was perpendicular to the rotation axis of the magnet by adjusting the sample to achieve superposition of appropriately related EPR lines. Reiterating these procedures several times, we were able to establish the crystal orientations with an accuracy of $\pm 0.05°$ for all rotation measurements. EPR spectra were recorded by varying the orientations of the external magnetic fields in three mutually perpendicular crystallographic planes with the polar angle θ and the azimuthal angle ϕ (measured from the $+c$- and $+a$-axis, respectively) ranging from zero to 180° at 3° intervals. Figure 2 displays an array of EPR spectra, the so-called 'stack-plot', measured in the crystallographic ca-plane at 3° intervals.

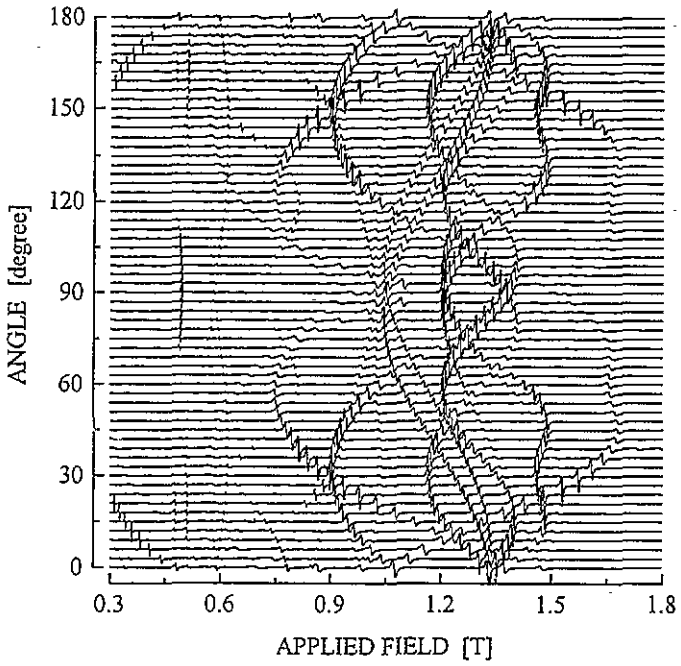

Figure 2. The angular dependence of the Fe^{3+} spectra in the ca-plane of $KTiOPO_4$ observed at the frequency 33.8616 ± 0.0003 GHz.

From the angular dependence of the EPR spectra, five allowed ($\Delta M_S = \pm 1$) and four forbidden ($\Delta M_S = \pm 2$) transitions between the spin states were clearly identified in each crystallographic plane. For an arbitrary orientation of the magnetic field with respect to the crystallographic axis, eight sets of the fine-structure lines were observed. The eight sets could be divided into two groups denoted as C1 and C2 which are related to the symmetry of the Fe^{3+} ion sites. Each group contains four sets of the fine-structure lines, which arise from the chemically equivalent but magnetically inequivalent Fe^{3+} ion sites. However, when the magnetic field was aligned in one of the three crystallographic planes, only two sets of the fine structures were recorded. These sets merged into one when the magnetic field was oriented along a crystallographic axis (see figure 2). In order to distinguish the degenerate pairs of EPR lines, the angular dependence was also measured with the magnetic field lying in three skew planes at 4° intervals, which deviated slightly (about $\pm 1 \sim 2°$ from the exact

ab-, *bc*- and *ca*-planes. The degenerate pairs of EPR lines for all four sites belonging to each group were split in the three skew planes.

3. Results and discussion

For the case of arbitrary low symmetry, EPR spectra of Fe^{3+} ($S = 5/2$) are described by a general spin Hamiltonian [2–4]:

$$H = \sum_{ij} \mu_B B_i g_{ij} S_j + \sum_{m=-2}^{2} B_2^m O_2^m + \sum_{m=-4}^{4} B_4^m O_4^m \tag{1}$$

where μ_B is the Bohr magneton, g_{ij} ($i, j = X, Y, Z$) the component of the **g**-tensor and O_n^m the extended Stevens operators [13]. From the angular dependence of the EPR spectra, we have newly identified four magnetically different Fe^{3+} sites belonging to each centre C1 and C2, which arise from the symmetry of the point group *mm*2 of KTP. These new sites have been named C1a, C1b, C1c and C1d for those belonging to the centre C1, and C2a, C2b, C2c and C2d for those belonging to the centre C2, where the sites C1a and C2a appear to correspond directly to the centres ST3 and ST2, respectively. For all Fe^{3+} sites, the 20 parameters of equation (1) are calculated by employing a computer program (EPR.FOR). In order to compare the present results with other experimental data [4], the D_{ij} values obtained directly from the program are converted to the extended Stevens operator notation [14] using the relations from [15].

All four Fe^{3+} sites belonging to each centre have identical principal values of the **g**-tensors and the second-order ZFS tensors within the experimental uncertainty, apart from the different orientations of the principal axes of the tensors. If the orientation of each principal axis of the tensors for the C1a (C2a) site is represented by the direction cosines lmn, the orientation of this axis for the site C1b (C2b) is given by $\bar{l}mn$, as follows from applying a reflection of the glide plane n to C1a (C2a). Similarily, for the site C1c (C2c) we obtain $l\bar{m}n$ by applying a reflection of the glide plane a to C1a (C2a). When the orientation of each principal axis for the C1a (C2a) site is given in a right-handed coordinate system, that for the sites C1b (C2b) and C1c (C2c) would be described by a left-handed one to satisfy the above-mentioned relation. The site C1d (C2d) can be obtained by successively applying the reflections of both glide planes n and a, or by applying a 180° rotation around the screw axis alone to C1a (C2a). It is possible to choose two sets of direction cosines for the site C1d (C2d): (i) $lm\bar{n}$ being represented by a left-handed coordinate system; or (ii) $\bar{l}\bar{m}n$ being represented by a right-handed one. The set of the direction cosines lmn, $\bar{l}mn$, $l\bar{m}n$ and $lm\bar{n}$ was chosen in some reports [6,7,9]. However, the site C1d (C2d) generated by

Table 1. The relative orientations of the principal axes of the **g**-tensor and second-order ZFS tensor for the four magnetically inequivalent Fe^{3+} sites belonging to the centres C1 and C2. The principal-axis orientations of the other three sites for each centre can be obtained from those for the representative sites C1a and C2a in tables 2 and 3.

Sites		Orientations of the principal axes		
C1	C2	θ (deg)	ϕ (deg)	Reflection planes
C1a	C2a	θ_1	ϕ_1	
C1b	C2b	θ_1	$180° - \phi_1$	n
C1c	C2c	θ_1	$360° - \phi_1$	a
C1d	C2d	θ_1	$180° + \phi_1$	Both n and a

Table 2. The principal values of the g-tensors and the orientations of their principal axes x', y', z' with respect to the crystallographic axes X, Y, Z for the representative sites C1a and C2a for the Fe^{3+} ions in KTP. The estimated statistical uncertainties in the last significant figures are given in parentheses.

	C1 (site C1a)		C2 (site C2a)	
Components	Principal values of g-tensors			
$g_{x'}$	2.002 69(15)		2.003 22(15)	
$g_{y'}$	1.999 49(12)		2.001 89(15)	
$g_{z'}$	1.998 22(15)		1.999 95(13)	
	Orientations (deg) of the principal axes			
	θ	ϕ	θ	ϕ
Ox'	76.0(1.7)	234.8(1.3)	74.6(2.2)	310.7(3.7)
Oy'	27.8(4.5)	116.5(5.1)	97.7(3.2)	38.5(3.8)
Oz'	113.5(4.5)	151.0(2.0)	17.3(2.7)	102.8(5.8)

Table 3. The principal values of the second-order ZFS tensors and the orientations of their principal axes x, y, z with respect to the crystallographic axes X, Y, Z for the representative sites C1a and C2a for the Fe^{3+} ions in KTP. The data of Gaite *et al* are included for comparison.

	Present work			
	C1 (site C1a)		C2 (site C2a)	
	Principal values of the second-order ZFS tensors[a]			
B_2^0 (cm^{-1})	−0.081 73		−0.073 91	
B_2^2 (cm^{-1})	−0.044 31		−0.044 22	
	Orientations (deg) of the principal axes of the second-order ZFS tensors[b]			
	θ	ϕ	θ	ϕ
Ox	102.17	7.99	112.16	78.15
Oy	148.58	118.65	39.99	139.09
Oz	61.52	91.28	58.65	2.51
	Gaite *et al*			
	ST3		ST2	
B_2^0 (cm^{-1})	−0.082 17		−0.074 07	
B_2^0 (cm^{-1})	−0.044 37		−0.044 29	
Ox	102.5	7.7	110.3	78.4
Oy	148.3	118.7	40.1	139.1
Oz	61.4	90.8	58.6	2.7

[a] The estimated maximum uncertainties are ±0.000 01 for all sites.
[b] The estimated maximum uncertainties in the angle are ±0.01 for all sites.

this proper transformation should be represented by the same kind of coordinate as that of C1a (C2a). When the orientation of each principal axis is described by the angles θ and ϕ, simpler relations among the four magnetically inequivalent Fe^{3+} sites for each centre can

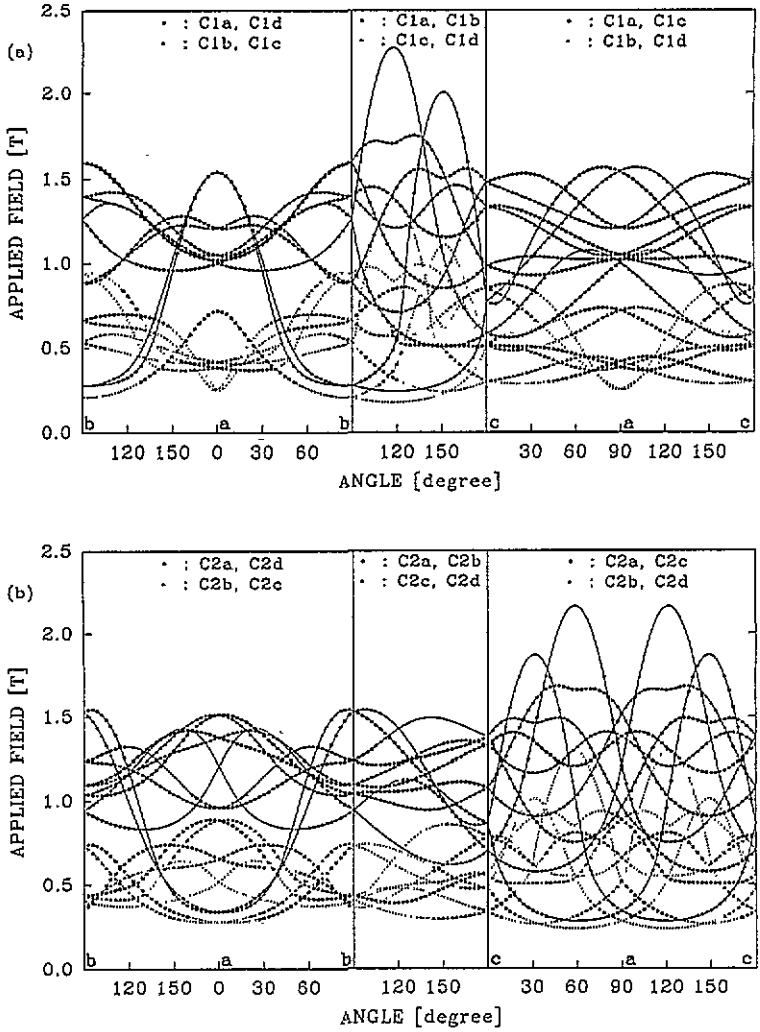

Figure 3. The angular dependence of the Fe^{3+} spectra in the *ab*-, *bc*- and *ca*-planes of $KTiOPO_4$, observed at 33.8673, 33.8647 and 33.8616 ± 0.0003 GHz, respectively: (a) For the C1 centre (b) for the C2 centre. The experimental points are represented by closed circles and triangles, whereas calculations are represented by full lines for the allowed transitions and dotted lines for the forbidden transitions.

be obtained from the set of direction cosines lmn, $\bar{l}mn$, $l\bar{m}n$ and $\bar{l}\bar{m}n$, as shown in table 1. The results in table 1 agree with those of [8]. These relations are consistent with the point symmetry among the four Ti^{4+} positions as described in figure 1. Therefore, it is possible to assign the positions I, II, III and IV to the sites C1a, C1b, C1c and C1d belonging to the centre C1, respectively. In the same way, the C2a, C2b, C2c and C2d sites belonging to the centre C2 can be correlated with the other set of four Ti^{4+} positions which have the same relations as shown in figure 1.

Since the four magnetically inequivalent sites for each Fe^{3+} centre arise from the crystal symmetry of KTP characterized by two glide planes n and a, any kind of defect centre with local site symmetry C_1 in KTP will have the four magnetically inequivalent sites and

Table 4. The spin-Hamiltonian parameters of the representative sites C1a and C2a for the Fe^{3+} ions in KTP in the crystallographic axes X, Y, Z. The data of Gaite *et al* are included for comparison.

	Present work		Gaite *et al*	
	C1 (site C1a)	*C2 (site C2a)*	*ST3*	*ST2*
ij	Matrix components g_{ij}[a]			
XX	1.999 67(11)	2.002 40(10)	1.9995	2.0027
YY	2.001 25(11)	2.002 44(11)	2.0055	2.0026
ZZ	1.999 47(10)	2.000 21(9)	2.0045	2.0056
XY	*0.001 87(14)*	*−0.000 57(14)*	*0.0050*	*0.0009*
XZ	−0.000 84(12)	0.000 34(9)	−0.0019	−0.0011
YZ	−0.000 39(10)	−0.000 80(15)	0.0000	−0.0008
m	Second-order ZFS parameters B_2^m (cm^{-1})[b]			
0	281.3	167.9	278.6	167.5
1	415.5	−2234.1	405.3	−2243.4
−1	−2375.4	501.2	−2398.2	492.9
2	710.2	−618.9	713.1	−617.0
−2	−66.8	−237.4	−81.9	−241.3
m	Fourth-order ZFS parameters $60B_4^m$ (cm^{-1})[b]			
0	28.8	24.4	28.0	21.7
1	20.4	46.0	19.6	44.9
−1	61.0	51.8	62.0	20.2
2	−227.9	215.3	−224.5	210.6
−2	−13.8	72.3	−21.9	76.9
3	31.6	−343.5	−30.1	−309
−3	363.7	90.2	379.8	113.8
4	−136.8	−88.5	−113.6	−71.0
−4	−11.1	−74.4	−17.2	−71.0

[a] The estimated statistical uncertainties in the last significant figures are given in parentheses.
[b] The estimated maximum uncertainties of B_2^m and $60B_4^m$ are ±0.1 for all centres.

their direction cosines will be given by the same relations as those of the Fe^{3+} sites as well as those found in some other reports [6–9]. However, when the local site symmetry of a paramagnetic ion in KTP is higher than C_1, the number of magnetically inequivalent sites will be reduced.

For the C1a and C2a sites, belonging to the centres C1 and C2 respectively, the principal values of the **g**-tensors and the orientations of their principal axes x', y', z' are summarized in table 2, where the axes x', y', z' are taken in the order of their magnitudes: $g_{x'} > g_{y'} > g_{z'}$. The principal values of the second-order ZFS tensors, and the orientations of their principal axes x, y, z are listed in table 3 together with the values previously reported [4]. We chose the principal axes to conform with the convention $|B_2^0| \geqslant |B_2^2|$ and the two parameters having the same sign [16].

The site-rotation matrices, which transform all symmetry-related sites into a reference site, could be found from the relations: lmn, $\bar{l}mn$, $l\bar{m}n$ and $\bar{l}\bar{m}n$. Using this matrix set for each centre, we have calculated two sets of the spin-Hamiltonian parameters that simultaneously fitted the data of the four sites for each centre. The values of g_{ij} and of the ZFS parameters for the sites C1a and C2a are listed in table 4, where the parameters are

given in the reference frame of a crystallographic axis system defined as $X = a$, $Y = b$ and $Z = c$. The standard deviations between the experimental and calculated magnetic transitions are 1.0 mT and 1.1 mT for the centres C1 and C2, respectively. In order to demonstrate the confidence that can be placed on the parameters determined, the calculated rotation patterns of the centres C1 and C2 in the *ab*-, *bc*- and *ca*-planes are displayed in figure 3 together with experimental data. The EPR lines for the four Fe^{3+} sites for each centre are differently degenerated into two pairs in the three crystallographic planes. The degenerate pairs in each plane are as follows: C1a (C2a) and C1d (C2d) as well as C1b (C2b) and C1c (C2c) in the *ab*-plane; C1a (C2a) and C1b (C2b) as well as C1c (C2c) and C1d (C2d) in the *bc*-plane; C1a (C2a) and C1c (C2c) as well as C1b (C2b) and C1d (C2d) in the *ca*-plane. In order to confirm the degenerate pairs of EPR lines, the spin-Hamiltonian parameters of all the sites split in the three skew planes were also calculated. When the degenerate pairs of all the Fe^{3+} sites for each centre were assigned as in figure 3, we were able to obtain the same results as those in tables 2, 3, and 4, within experimental uncertainty. The nondegenerate pairs have mirror symmetry to each other about the *a*-, *b*- and *c*-axes in each crystallographic plane.

Using the pseudosymmetry axis method [17, 18], it was found that the centres were due to the Fe^{3+} ion at Ti(1) for ST3, and at Ti(2) for ST2 [4]. As displayed in table 3 and 4, the centres C1 and C2 are equivalent to ST3 and ST2, respectively. In addition to this result, eight Fe^{3+} sites can be determined by comparing the orientions of the principal axes with the symmetry relations among the four crystallographically equivalent Ti^{4+} positions, as shown in figure 1. The sites C1a, C1b, C1c and C1d belonging to the C1 centre are due to the Fe^{3+} ions replacing Ti(1) at the I, II, III and IV positions, respectively. On the other hand, the sites C2a, C2b, C2c and C2d belonging to the C2 centre are due to the Fe^{3+} ions replacing Ti(2) at the I, II, III and IV positions, respectively. When all the Fe^{3+} sites for each centre are assigned in this way, the degenerate aspects of the EPR lines in the three crystallographic planes, as shown in figure 3, are also consistent with those of the four chemically equivalent but magnetically inequivalent Ti^{4+} positions for each kind of titanium.

Acknowledgments

This work was supported by the Korea Science and Engineering Foundations through the Research Centre for Dielectric and Advanced Matter Physics (RCDAMP) at Pusan National University. One of the authors (S W Ahn) is grateful to City University of Hong Kong for the Research Assistantship and to Professor C Rudowicz for critically reading the manuscript. The computer program 'EPR version 5.13' (authors: D G McGavin, M Y Mombourquette and J A Weil, Department of Chemistry, University of Saskatchewan, Canada) has been employed.

References

[1] Zumsteg F C, Bierlein J D and Gier T E 1976 *J. Appl. Phys.* **47** 4980
[2] Nizamutdinova N M, Khasanova N M, Bulka G R, Vinokurov V M, Rez I S, Garmash V M and Pavlova N I 1987 *Sov. Phys.–Crystallogr.* **32** 408
[3] Stenger J F, Dusausoy Y, Marnier G, Rager H and Gaite J M 1989 *J. Phys.: Condens. Matter* **1** 4643
[4] Gaite J M, Stenger J F, Dusausoy Y, Marnier G and Rager H 1991 *J. Phys.: Condens. Matter* **3** 7877
[5] Tordjman I, Masse R and Guitel J C 1974 *Z. Kristallogr.* **139** 103
[6] Han S, Wang J, Xu Y, Liu Y and Wei J 1992 *J. Phys.: Condens. Matter* **4** 6009
[7] Bravo D, Martin M J, Gavalda J, Diaz F, Zaldo C and Lopez F J 1994 *Phys. Rev.* B **50** 16224

[8] Edwards G J, Scripsick M P, Halliburton L E and Belt R F 1993 *Phys. Rev.* B **48** 6884
[9] Ahn S W, Choh S H and Kim J N 1995 *J. Phys.: Condens. Matter* **7** 667
[10] Ahn S W, Choh S H, Choi B C and Kim J N 1994 *Ferroelectrics Lett.* **18** 203
[11] Bolt R J, De Hass H, Sebastian M T and Klapper H 1991 *J. Cryst. Growth* **110** 587
[12] Choi B C, Kim J B, Yun S I and Kim J N 1993 *Korean Appl. Phys.* **6** 27
[13] Rudowicz C 1985 *J. Phys. C: Solid State Phys.* **18** 1415
[14] Rudowicz C 1987 *Magn. Reson. Rev.* **13** 1
[15] McGavin D G 1987 *J. Magn. Reson.* **74** 19
[16] Rudowicz C and Bramley R 1985 *J. Chem. Phys.* **83** 5192
[17] Michoulier J and Gaite J M 1972 *J. Chem. Phys.* **56** 5205
[18] Gaite J M and Michoulier J 1973 *J. Chem. Phys.* **59** 488